Check for updates

Microbial assemblages and associated biogeochemical processes in Lake Bonney, a permanently ice-covered lake in the McMurdo Dry Valleys, Antarctica

Hanbyul Lee[1], Kyuin Hwang[1], Ahnna Cho[1], Soyeon Kim[1], Minkyung Kim[1], Rachael Morgan-Kiss[2], John C. Priscu[3], Kyung Mo Kim[1] and Ok-Sun Kim[1*]

Abstract

Background Lake Bonney, which is divided into a west lobe (WLB) and an east lobe (ELB), is a perennially ice-covered lake located in the McMurdo Dry Valleys of Antarctica. Despite previous reports on the microbial community dynamics of ice-covered lakes in this region, there is a paucity of information on the relationship between microbial genomic diversity and associated nutrient cycling. Here, we applied gene- and genome-centric approaches to investigate the microbial ecology and reconstruct microbial metabolic potential along the depth gradient in Lake Bonney.

Results Lake Bonney is strongly chemically stratified with three distinct redox zones, yielding different microbial niches. Our genome enabled approach revealed that in the sunlit and relatively freshwater epilimnion, oxygenic photosynthetic production by the cyanobacterium *Pseudanabaena* and a diversity of protists and microalgae may provide new organic carbon to the environment. CO-oxidizing bacteria, such as Acidimicrobiales, Nanopelagicales, and Burkholderiaceae were also prominent in the epilimnion and their ability to oxidize carbon monoxide to carbon dioxide may serve as a supplementary energy conservation strategy. In the more saline metalimnion of ELB, an accumulation of inorganic nitrogen and phosphorus supports photosynthesis despite relatively low light levels. Conversely, in WLB the release of organic rich subglacial discharge from Taylor Glacier into WLB would be implicated in the possible high abundance of heterotrophs supported by increased potential for glycolysis, beta-oxidation, and glycoside hydrolase and may contribute to the growth of iron reducers in the dark and extremely saline hypolimnion of WLB. The suboxic and subzero temperature zones beneath the metalimnia in both lobes supported microorganisms capable of utilizing reduced nitrogens and sulfurs as electron donors. Heterotrophs, including nitrate reducing sulfur oxidizing bacteria, such as Acidimicrobiales (MAG72) and Salinisphaeraceae (MAG109), and denitrifying bacteria, such as *Gracilimonas* (MAG7), Acidimicrobiales (MAG72) and Salinisphaeraceae (MAG109), dominated the hypolimnion of WLB, whereas the environmental harshness of the hypolimnion of ELB was supported by the relatively low in metabolic potential, as well as the abundance of halophile *Halomonas* and endospore-forming *Virgibacillus*.

Conclusions The vertical distribution of microbially driven C, N and S cycling genes/pathways in Lake Bonney reveals the importance of geochemical gradients to microbial diversity and biogeochemical cycles with the vertical water column.

Keywords Hypersaline, Cryosphere, Metagenomics, Biogeochemical cycles, Microbial metabolism

*Correspondence:
Ok-Sun Kim
oskim@kopri.re.kr
Full list of author information is available at the end of the article

BMC

Lee *et al. Environmental Microbiome*   (2024) 19:60

Page 2 of 15

Background

The McMurdo Dry Valleys (MDVs) form the largest ice-free region of Antarctica and are considered a polar desert characterized by consistent subzero temperatures, low precipitation, extreme light/dark cycles, and the absence of higher plants and macroscopic animals [1–3]. Lake Bonney, a permanently ice-covered lake in the upper Taylor Valley, is one of the most hydrologically stable and geochemically unique lake ecosystems in Antarctica (Fig. 1) [4–7]. The lake is divided into two distinct lobes with maximum depth of about 40 m separated by a shallow sill that limits the exchange of water and associated microorganisms and geochemical constituents to the layers above the chemocline [6, 8].

According to previous studies, the food web is dominated by photosynthetic microalgae, protists, bacteria, heterotrophic flagellates, fungi and viruses driven largely by sunlight that penetrates the permanent ice cover for approximately 6 months each year [3, 9–12]. The lake has no outflow and receives water from low nutrient glacial melt streams that flow between 4–6 weeks each summer. The west lobe of the lake also receives hypersaline, iron-rich subglacial discharge at the terminus of Taylor Glacier that directly influences the physical and geochemical properties of this lobe [6, 13–15]. Phytoplankton in the upper euphotic waters of the epilimnion are highly P-deficient [16, 17]. The epilimnion is supersaturated with oxygen that originates primarily from gas segregation during lake ice formation, with suboxic levels present beneath the chemocline [3, 18]; the permanent ice cover leads to low atmospheric ventilation [19]. Measurable heterotrophic denitrification occurs in the deep suboxic waters of the WLB but not the deep suboxic water of ELB [20–22]. High levels of biogenic sulfur compounds are present in both lobes [23].

The ecological role of prokaryotic microorganisms is important in Lake Bonney and other MDV lakes because they contain a paucity of metazoans [3, 10, 24]. Kwon et al. [10] demonstrated, through 16S rRNA amplicon analysis, that Bacteroidetes, Actinobacteria, and Pseudomonadota are the predominant phyla in Lake Bonney constituting over 85% of the microbial composition [24]. Alphaproteobacteria were prevalent throughout the water column in ELB whereas the dominant taxa varied with depth in WLB; Actinobacteria were predominant in the epilimnion, while Gammaproteobacteria were more prevalent below the chemocline. Although various studies have reported on the microbial diversity of MDVs including Lake Bonney [11, 12, 25, 26], there are limited reports on the direct association with biogeochemical functions. Here we present metagenomic data from Lake Bonney in order to evaluate metabolic potential and the contribution of microorganisms to biogeochemical cycling along physicochemical gradients. Our comprehensive analyses included both gene- and genome-centric approaches to reconstruct depth-gradient functional profiles and to reveal the diversity of metagenome-assembled genomes (MAGs), respectively.
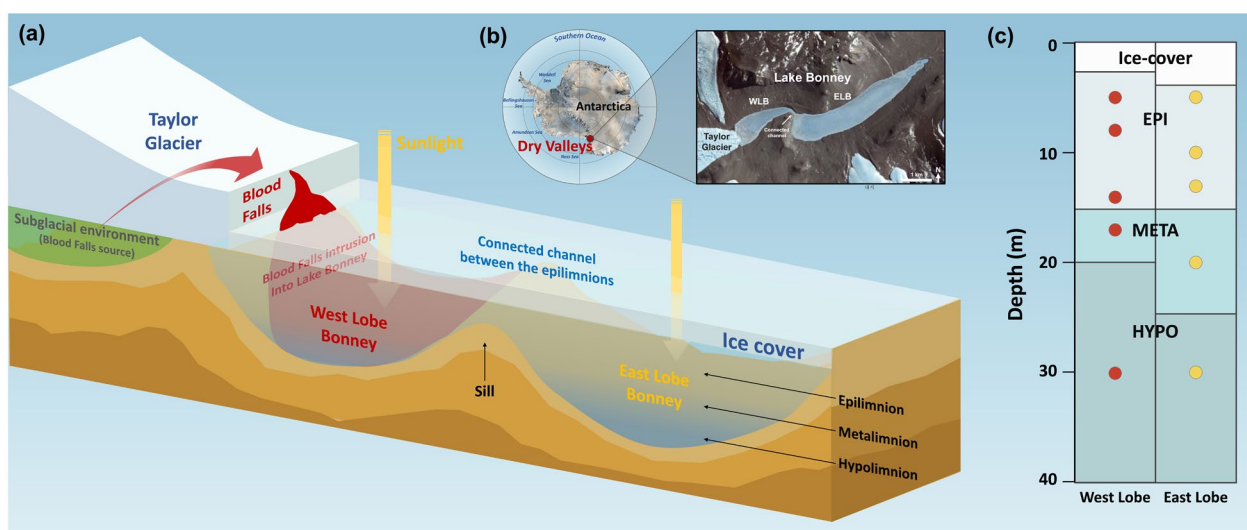

Fig. 1 Conceptual diagram of Lake Bonney showing the subglacial intrusion (Blood Falls) and vertical zonation (**a**) together with a satellite image and locator map (**b**) the lake, and the depth of stratified layers and sampling points (**c**). The strong chemocline occurs within the metalimnetic layer of both lobes

Lee *et al. Environmental Microbiome*   (2024) 19:60

Page 3 of 15

Materials and methods

Sample collection and physicochemical properties

Samples were collected from WLB ($-77°42'$S $162°17'$E) and ELB ($-77°44'$S $162°10'$E) during November 2017. A total of 10 water samples from WLB (5, 8, 14, 17, 30 m) and ELB (5, 10, 13, 20, 30 m) were collected using a 5 L Niskin water sampler. These depths represent regions of distinct geochemical redox gradients within the lake [18, 23, 27]. Upon collection, the samples were sealed and immediately transported to a field laboratory where 1 L was filtered under gentle vacuum onto a 0.2 µm PES filter (PALL Corporation, USA) for metagenome analysis. Filters were shipped frozen to our laboratory at Korea Polar Research Institute on dry ice and then stored at -80 °C until genomic DNA extraction.

Physicochemical properties were measured according to the procedures outlined in the MCM LTER lake manual (http://www.mcmlter.org/data/mcm-lter-data-file-format-protocols-database-submission), briefly summarized below. Temperature and conductivity were measured with an SBE 25 Sealogger CTD. Dissolved oxygen (DO) was measured using the azide modification of the mini-Winkler titration. Underwater photosynthetically active radiation (PAR) was measured using a LI-COR LI-193SA spherical quantum sensor (LI-COR Biosciences) near 12 PM local time. Macronutrients (NH_4^+, NO_3^-, NO_2^-) were analyzed as described by Priscu [16]. Dissolved organic carbon (DOC) was determined using a Shimadzu TOC-V series total organic carbon (C) analyzer on GF/F filtered and acidified samples. Dissolved inorganic carbon was measured on acid-sparged samples using infrared spectroscopy, and particulate organic carbon (POC) and particulate organic nitrogen (PON) were measured on acidified samples using a Thermal-Finnigan elemental analyzer calibrated with acetanilide.

DNA extraction and sequencing

Genomic DNA was extracted using a FastDNA® SPIN kit (MP Biomedicals, Illkirch, France) after cutting the filter paper into several pieces. DNA libraries for sequencing were prepared with a TruSeq Nano DNA Library Prep Kit (Illumina, USA) following the manufacturer's instructions. Shotgun metagenomic sequencing was conducted by LAS Inc. (Gimpo, Korea) using the Illumina MiSeq platform (300 bp paired-end).

The gene-centric approach for microbial community analysis and depth gradient functional profiles

For the gene-centric analysis, the raw metagenomic sequence reads were quality filtered using Trimmomatic v.0.39 (LEADING:3 TRAILING:3 SLIDINGWINDOW:4:15 MINLEN:38) [28]. Reads with low complexity, defined as those containing less than 5% of any nucleotide, were excluded from the analysis. The reads were then mapped to a human reference genome (GRCh38) using BWA v0.7.17 [29]. The filtered reads were assembled for the each of ten water samples using Megahit v.1.2.9 [30]. Contigs with less than 500 bp were discarded, and then open reading frames (ORFs) were predicted using Prodigal v.2.6.3 [31] in metagenome mode. The protein sequences of the ORFs were submitted to the GhostKOALA server v.2.2 (http://www.kegg.jp/ghostkoala/) to retrieve KEGG orthology (KO) [32] for each gene. The glycoside hydrolase family was assigned to KOs belonging to the subfamily EC 3.2.1 in the KEGG enzyme database. The peptidases were assigned to the KOs marked as the MEROPS family [33]. Genes related to iron oxidation/reduction were annotated using the FeGenie v.1.0 [34]. The genes assigned as the dissimilatory sulfite oxidase large subunit (*dsrA*, K11180) facilitate either sulfide oxidation or sulfite reduction. To distinguish these genes, we compared and analyzed DsrA sequences obtained from public databases [35, 36] with those obtained from our study. These DsrA sequences were aligned using ClustalW v2.1 [37] and analyzed through a maximum-likelihood phylogenetic tree constructed with RAxML v8.2.12 [38], using 100 bootstrap replicates and a model from ModelTest-NG [39]. Based on the tree topology, the DsrA sequences were categorized by their predominant catalytic activities, either sulfide oxidation or sulfite reduction. The forward reads of each sample were mapped on assembled contigs of same sample using Bowtie2 v.2.4.4 [40], and the number of mapped reads was counted for KO genes. The reverse reads, with generally low quality and shorter length, were not used here. To avoid ambiguity, reads overlapping with two more successive genes on a contig were excluded from calculation. To estimate the metabolic potential for each sample, we followed the methods described by Alneberg et al., [41]. Reads per million (RPM) were calculated by normalizing the read number using both gene lengths and total mapped read number. The RPM with the same KO was summed to obtain the abundance of each KO.

The genome-centric approach for the reconstruction of metagenome-assembled genomes and their functional profiles

The filtered reads were co-assembled for samples from each lobe using Megahit v.1.2.9 [30]. The contigs were binned individually using MaxBin2 v.2.2.7–3 [42], MetaBat2 v.2.15 [43], and Concoct v.1.1.0 [44]. We consolidated the bins generated by these three different tools using DASTool v.1.1.3 [45]. We dereplicated these MAGs using dRep v.3.0.0 with the default settings [46]. Genome quality was estimated using CheckM v.1.1.3

[47] and DAStool. A set of medium- and high-quality genomes was chosen by applying ≥ 50% completeness and < 5% contamination [48]. To calculate the percentage of filtered reads used in MAGs, the filtered reads for each sample were mapped to the MAGs using Bowtie2 v.2.4.4 [40], and the proportion of mapped reads was subsequently calculated. Taxonomic classification of the genomes was determined using GTDB-tk v.1.7.0 [49]. The phylogenetic tree was reconstructed using MEGA X v.10.1.8 [50] with the maximum-likelihood method with the alignment of 120 concatenated bacterial gene markers from GTDB-Tk. The phylogenetic confidence was evaluated using the bootstrap method with 100 replicates. All phylogenetic trees were visualized using iTOL v.6.6 [51]. To calculate coverage and reads per kilobase of contig per million reads (RPKM), we used Coverm v.0.6.1 available at https://github.com/wwood/CoverM. The potential metabolic pathway for each genome was estimated by the completeness of the pathway based on the KEGG-decoder [52]. In addition, all MAGs were analyzed using the FeGenie v.1.0 to identify iron-related genes [34]. To determine the presence of a metabolic pathway, each MAG must possess key enzymes for that pathway. In cases involving multistep processes, such as glycolysis, gluconeogenesis, or the TCA cycle, the genome must contain more than 50% of the gene set involved in the process, based on the KEGG module, including all key enzymes (Supplemental Table S1).

Results

Physicochemical profiles

Lake Bonney abuts Taylor Glacier in the Taylor Valley, approximately 60 km inland from McMurdo Sound (Fig. 1). Raw data from both lobes of the lake are publicly available with Digital Object Identifiers (DOI) on the McMurdo Dry Valleys LTER website (https://mcm.lternet.edu/limnological-data). During the summer (November) of 2017 ice thicknesses was 4.55 m and 3.95 m in the WLB and ELB, respectively. The water column of Lake Bonney is highly stratified with relatively freshwater (conductivity < 15 mS cm^{-1}) above 15 m [8] in both lobes. Conductivity in WLB formed a sharp chemocline between 15 and 20 m; conductivity beneath the chemocline exceeded 75 mS cm^{-1} (Supplemental Fig. S1). A chemocline was also present in the ELB between 15 and 25 m with conductivity levels > 110 mS cm^{-1} below 25 m. Accordingly, we defined the metalimnion of the ELB and WLB based on conductivity, with depths ranging from 15–20 m and 15–25 m, respectively. The layers above and below the metalimnion were classified as the epilimnion and hypolimnion, respectively. Water temperature near the ice-cover was close to 0 °C and gradually increased with depth, reaching 3.8 °C at 10 m in WLB and 4.6 °C

at 16 m in ELB. Subsequently, the temperature dropped sharply at the metalimnion in WLB, while in ELB it decreased more gradually, reaching minimum temperatures of approximately − 4 °C and -2 °C in the hypolimnia in the WLB and ELB, respectively. DO reached supersaturated levels of 48.9 mg L^{-1} and 42.6 mg L^{-1} just above the metalimnia in WLB and ELB, respectively, and decreased to suboxic levels (< 1 mg L^{-1}) beneath the metalimnia. pH ranged from 5.7 to 8.9 and from 6.1 to 8.5 in WLB and ELB, respectively, and decreased with depth in both lobes. PAR continuously decreased with depth, showing no layers of significant turbidity. The bottom of the trophogenic zone (i.e., zone where PAR no longer supports phytoplankton photosynthesis) occurs at approximately 20 m in each lobe [16]. Chl-*a* was bimodally distributed down the water columns of both lobes, with peak levels occurring just beneath the ice cover and near the metalimnion. The Chl maxima coincide with peaks in phytoplankton primary productivity [16].

Particulate organic carbon (POC) was relatively high beneath the metalimnia of both lobes. POC concentrations were 2 to threefold higher beneath the metalimnia of WLB and ELB at 46.6 and 47.4 mM, respectively, compared to levels immediately below the ice cover, which were measured at 17.2 and 14.1 mM. This trend also occurred for PON yielding average POC:PON molar ratios of 14.2 and 11.8 for WLB and ELB, respectively. DOC also decreased beneath the metalimnia, reaching 2.4 mM near the bottom of the ELB during our study. As with DOC, DIC increased below the metalimnion, exceeding 60 mM near the bottom of the WLB. Dissolved inorganic N and P were typically low (N < 10 µM; P < 0.1 µM) above the metalimnion. Nitrate was below detection (< 0.05 µM) in the deep waters of the WLB. Levels of nitrite and nitrate in ELB remained high (> 40 µM) beneath the metalimnion. Sulfate was high in the suboxic waters of both lobes of Lake Bonney, and no hydrogen sulfide was detected. The lack of sulfate and nitrate reduction in these suboxic waters has been discussed previously [19, 23].

Metabolic potential with depth reconstructed by gene-centric analysis

For the gene-centric analysis of 10 samples, we first identified 5 million ORFs from 12 million contigs that were assembled from 83 million raw reads (Supplemental Table S2). Thirty percent of the ORFs were assigned to 14,067 KOs using the KEGG database (Supplemental Table S2). For every sample, approximately 2.6 million reads were mapped to the assigned ORFs of KOs to calculate RPM of a KO. Here, we evaluated the metabolic potential of the microbial community in a sample using RPM of corresponding KOs (Supplemental Table S3).

Metabolic potentials varied with depth. For example, photosynthesis and aerobic CO oxidation were prominent in the epi- and metalimnia, whereas genes for the oxidation of sulfide and thiosulfate as well as reduction by denitrification and dissimilatory nitrate reduction to ammonia (DNRA) were prominent in the hypolimnia (Fig. 2).

The metabolic potential of the Calvin-Benson-Bassham cycle (CBB) was detected in Lake Bonney using the key enzyme *rbcL*, whereas other carbon fixation pathways were not found. The maximum RPMs of *rbcL* (K01601)

were observed at 5 m in the WLB (281.8) and 20 m in the ELB (164.0), with overall decreasing trends with depth in both lobes (Fig. 2, Supplemental Fig. S2 and Table S3). Major photosystem reaction center proteins for photosystems II and I, encoded by *psbB* and *psaA*, respectively, exhibited vertical trends similar to *rbcL*.

For glycolysis, the potential of Embden–Meyerhof–Parnas (EMP, *pfkA*, K00850) increased with depth in WLB, while that of Entner–Doudoroff (ED, *eda*, K01625) decreased with depth in ELB; these relationships did not exist in the EMP of ELB and ED of WLB. Throughout the

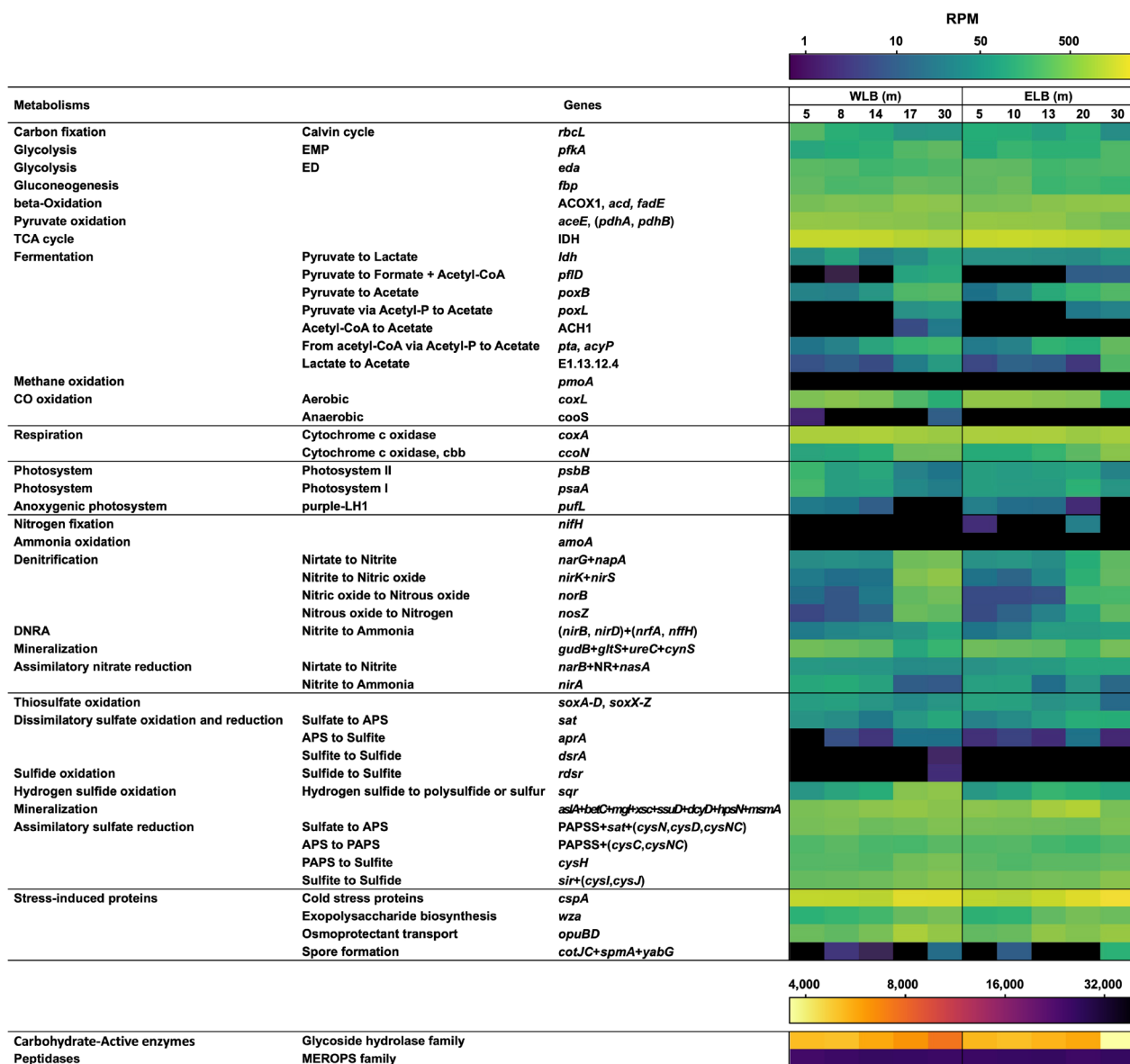**Fig. 2** Comparison of the functional differences in KEGG orthologous groups along the water columns. To estimate metabolic potential, reads per million (RPM) was calculated by normalizing the read number using both gene lengths and total mapped read number. The potential for each pathway was calculated by the sum or average of key enzymes involved in the pathway. The list of key enzymes is shown in Supplemental Table S3

Lee *et al. Environmental Microbiome*   (2024) 19:60

Page 6 of 15

water column, the ED pathway (257.6 RPM in WLB and 274.9 in ELB, on average) was more dominant than EMP (201.0 in WLB and 185.3 in ELB) in both lobes. Gluconeogenesis potential (*fbp*, K03841) was similar between WLB (305.9) and ELB (265.4) without notable change with depth. Beta-oxidation (K00232) reached maximum RPMs at 17 m in the WLB (656.3) and at 30 m in the ELB (673.1).

The decomposition of complex carbohydrates was measured by RPMs of glycoside hydrolase (GH) families (Supplemental Table S4). GH families increased with depth in WLB (5073.5–7422.1 RPMs). ELB retained a constant level with depth (ca. 5000 RPM); although, the potential decreased notably at 30 m (3503 RPM). Conversely, the potential for peptidases was relatively high and showed similar RPMs in both lobes regardless of sampling depth (Supplemental Tables S5).

The potential for the TCA cycle (K00031, *IDH*) decreased with depth in both lobes (1360.0–1022.3 in WLB and 1430.8–1125.7 RPM in ELB). The metabolic potential of CO oxidation (K03520, *coxL*) was relatively high in surface waters and decreased with depth in both lobes. The potential for CO oxidation in the epilimnia was higher in ELB (646.1) relative to WLB (535.0). The aa_3-type cytochrome c oxidase (low oxygen affinity; K02274, *coxA*) was abundant in all layers of the water column in both lakes (916.4 RPM in WLB and 911.9 in ELB, on average). Conversely, the metabolic potential for cbb_3-type cytochrome c oxidase (high oxygen affinity; K00404, *ccoN*) increased with depth in both lobes, although this gene was less abundant than the aa_3-type.

The metabolic potential of genes that are involved in a variety of fermentation steps from pyruvate to acetate typically increased with depth. Pyruvate fermentation to lactate (K00016, *ldh*), acetate (K00156, *poxB*), and formate and acetyl-CoA (K00656, *pflD*) showed higher potential in WLB (63.1, 133.8, and 47.0 RPMs, respectively) compared with ELB (53.6, 128.0, and 3.4). Specifically, acetate could be produced via other fermentation pathways, such as fermentation from acetyl-CoA (K01067, *ach1*), acetyl-P (K13788, *pta*), and lactate (K00467). Genes involved in methanogenesis and methane oxidation (e.g., K01944, *pmoA*) were not detected in any samples from the water column. The metabolic potential of genes related to iron oxidation and reduction exhibited markedly low metabolic potential in both lobes (Supplemental Table S6). In WLB, the potential for iron oxidation was detected only above the metalimnion, while the potential for iron reduction was detected at and below the metalimnion. In ELB, iron oxidation was detected at the epilimnion and metalimnion, with the potential for iron reduction identified exclusively at the metalimnion.

The metabolic potential for nitrogen cycling was higher in suboxic samples from beneath the metalimnia. No potential for nitrification (K10944, *amoA*) was detectable in either lobe, while a very low potential for nitrogen fixation (K02588, *nifH*) was detected at 20 m of ELB (26.1 RPM). Conversely, the potential for denitrification was relatively high, particularly in the WLB. Specifically, nitrate reduction (K00370, *narG* and K02567, *napA*) showed higher potential at a depth of 30 m in WLB (457.6 RPM) than ELB (312.2). Nitrite reduction (K00368, *nirK* and K15864, *nirS*) also showed a twofold higher potential at 30 m in WLB (656.1 RPM) compared with the same depth in the ELB (334.6). The potential of nitric oxide reduction (K04561, *norB*) was also higher in the hypolimnion of WLB (425.8 RPM) than that of ELB (249.6). Nitrous oxide reduction (K00376, *nosZ*) showed similar levels of potential in WLB (315.0 RPM) and ELB (314.0) at 30 m depth. The metabolic potential for producing ammonia via DNRA increased with depth in both lobes. Finally, the mineralization pathway that converts organic nitrogen into ammonia (K00260, *gudB*, K00284, *gltS*, K01428, *ureC*, and K01725, *cynS*) was the most prominent N cycle pathway in Lake Bonney.

Within the sulfur cycle, sulfide:quinone oxidoreductase (K17218, *sqr*) and mineralization showed high potential in both lobes. The potential of dissimilatory sulfite reduction (K11180, *dsrA*) and sulfide oxidation (K11180, *rdsrA*) were not detected in ELB, while a very weak potential for these reactions was measured at 30 m in WLB. Potential for elemental sulfur reduction to hydrogen sulfide (K17219-K17221, *sreABC*) was also not detected in Lake Bonney. The RPM value for hydrogen sulfide oxidation to elemental sulfur (K17218, *sqr*) increased at 17 m (570.7 RPM) and 30 m (644.2) of WLB but remained low throughout the water column of ELB. The potential for conversion (K00958, *sat*) of sulfate to adenosine-5'-phosphosulfate (APS) was higher at the hypolimnion in ELB (153.0 RPM) than in WLB (119.9 RPM), while the potential for subsequent reaction by adenylylsulfate reductase (K00394, *aprA*) was low at the hypolimnia in both lobes (15.4 RPM in WLB and 1.7 in ELB). The potential for thiosulfate oxidation by the *SOX* complex, including *soxABCD* and *soxXYZ*, was present across all depths of WLB and ELB. Assimilatory sulfate reduction showed that the potential was high in all samples of WLB and ELB. In addition, the mineralization of sulfur (K01130, *aslA*, K01133, *betC*, K01761, *mgl*, K03852, *xsc*, K04091, *ssuD*, K05396, *dcyD*, K15509, *hpsN*, and K16968, *msmA*) showed high potential through all samples from both lobes, and the highest potential was observed at 20 m in the ELB (1,060.2 RPM).

The metagenomic analysis mined numerous genes encoding stress-induced proteins that may help

microorganisms survive the harsh conditions of Lake Bonney. These proteins are associated with cold shock (K03704, *cspA*), exopolysaccharide biosynthesis (K01991, *wza*), osmoprotectant transport (K05846, *opuBD*), and spore formation (K06334, *cotJC,* K06373, *spmA,* and K06436, *yabG*) (Fig. 2. and Supplemental Table S3). *cspA*, a representative cold-induced protein, was abundant in both lobes, rapidly increased at the metalimnia, and showed the highest value at 30 m in ELB (2,479.7 RPM). The abundance of genes involved in the transport system for osmoprotectant (K05846, *opuBD*) reached high levels, measuring 975.3 RPM at the metalimnion of WLB and 766.1 at the hypolimnion of ELB, respectively. The abundance related to cryo- and osmo-protection production was not consistent with the salinity and temperature profiles of the lake. Interestingly, genes involved in spore formation were highly abundant at 30 m depth in ELB (175.1 RPM), which was 13-fold higher than that of WLB (13.3).

Metabolic potential inferred by the genome-centric approach

An array of metagenomic sequencing, co-assembly and binning resulted in 189 MAGs. They were then dereplicated and quality-filtered using the genomic recovery threshold of > 50% completeness and < 5% contamination [48], finally producing 120 medium- to high-quality MAGs (Fig. 3 and Supplemental Fig. S3). The completeness and contamination were averaged at 88.5% ± 11.3 and 2.2% ± 1.3, respectively (Supplemental Table S7). Among the total 120 MAGs, 58 were generated from the co-assembled contigs across the WLB samples, while 62 were generated from the co-assembled contigs across the ELB samples. Mapping the filtered reads to the MAGs revealed that an average of 70.5% of the filtered reads were utilized in the generation of MAGs. The MAGs represented 1 Archaea and 119 Bacteria that were classified into 13 phyla, 21 classes, and 74 orders. The MAGs were dominated by the phyla Bacteroidota (31 MAGs) and Pseudomonadota (31), followed by Acidobacteriota (19), Planctomycetota (14), and Verrucomicrobiota (12). The only archaeal MAG was classified to the phylum Halobacteriota.

Almost all MAGs have the potential to degrade complex organic molecules (e.g., glycoside hydrolase found in 119 MAGs and peptidase in 120 MAGs) (Supplemental Tables S8 and S9). Organotrophs possessing glycolysis (105 MAGs) and the TCA cycle (108) were highly abundant in the Lake Bonney water column (Fig. 3). MAGs capable of gluconeogenesis were detected in Bacteroidota (27 MAGs), Pseudomonadota (9), Gemmatimonadota (3), and other minor groups. Conversely, gluconeogenesis was absent in several taxonomic groups, including

Patescibacteria and Verrucomicrobiota, and Actinobacteria. Among taxa lacking gluconeogenesis, Verrucomicrobiota had relatively diverse glycoside hydrolase coding genes (Fig. 3). A total of 74 MAGs potentially capable of beta-oxidation were found in diverse taxonomic groups, and they were relatively evenly distributed across water depth. A total of 112 MAGs had aa_3-type cytochrome c oxidase, while the cbb_3-type exhibiting high oxygen affinity was relatively rare in 41 MAGs. The 29 MAGs capable of aerobic CO oxidation were affiliated with Pseudomonadota (13), Actinobacteria (10), Bacteroidota (3), Chloroflexota (2), and Archaea (1).

Only two MAGs (MAG66 from ELB and MAG67 from WLB) belonging to *Pseudanabaena* (Cyanobacteria) exhibited the potential for photosynthesis (*psbA* and *psaA*) and carbon fixation (the CBB pathway by *rbcL*); however, the *nifH* gene for atmospheric nitrogen fixation was absent in these genomes. Cyanobacterial MAGs were abundant in the epilimnia of both lobes (36.0 and 26.3 RPKMs at 5 and 10 m of ELB, respectively; 57.9 and 24.9 RPKMs at 5 and 8 m of WLB, respectively) but extremely rare in deeper layers (Supplemental Table S7). The five MAGs showing potential for iron oxidation were mostly from WLB and belonged to Verrucomicrobiota (2), Chloroflexota (2), and Pseudomonadota (1) whereas the potential for iron reduction was only observed in MAG87 assigned to the genus *Geopsychrobacter* in Thermodesulfobacteriota, which was almost exclusively found at a 30 m in WLB (16.4 RPKM in Supplemental Table S7). Consistent with the gene-centric analysis, the potential for methane oxidation was not detected in the MAG data.

The capability of nitrogen fixation existed in only two MAGs that are affiliated with *Mariniblastus* of Planctomycetota. They were relatively prominent at 14 m in the WLB (2.0 RPKM) and 13 m in ELB (4.2 RPKM); however, the overall abundance (3.5 and 7.5 RPKM, respectively) was low. The metabolic potential of nitric oxide reduction and nitrous oxide reduction that are involved in denitrification was observed in 20 MAGs and 14 MAGs, respectively, and were mostly present at or below the metalimnia of both lobes. Specifically, MAG34 of WLB (143.4 RPKM at 17 m and 81.7 at 30 m) and MAG115 of ELB (186.1 RPKM at 30 m) that are affiliated with Flavobacteriaceae and *Halomonas,* respectively, showed high abundance at the hypolimnion of each lobe. The potential of nitrite reduction to ammonia was detected in 30 MAGs that were distributed across diverse taxonomic phyla and were more abundant above the metalimnia of both lobes. Evidence for nitrification was not detected in the MAG data, which agreed with results from the gene-centric approach. The potential of N mineralization was observed in 56 MAGs and was detected at all depths of
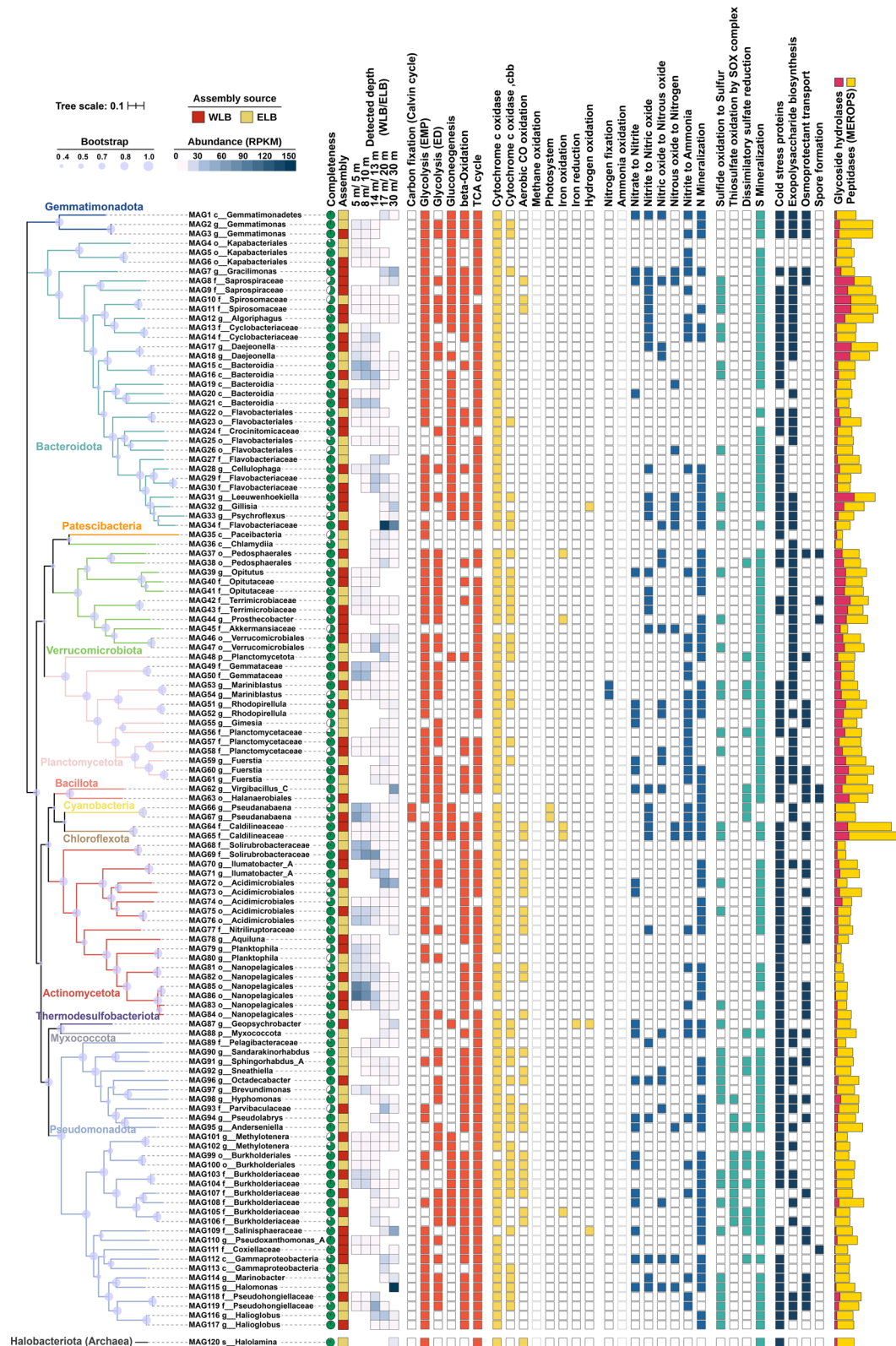
Fig. 3 Phylogeny and the potential of each function for the 120 MAGs recovered from Lake Bonney. The potential of each function was estimated by the presence of key enzymes involved in the metabolic pathways using the KEGG-Decoder

the water column of both lobes. N mineralization potential was observed more frequently in Pseudomonadota, followed by Actinomycetota and Bacteroidota.

A total of 20 MAGs, which have *sat* (K00958) and/or *aprA* (K00394), exhibited potential for dissimilatory sulfate reduction; however, none of the MAGs contained either the *dsrA* or *rdsrA* genes. A total of 41 MAGs with *sqr* were mostly affiliated with Pseudomonadota and Bacteroidota and were distributed evenly across sampling depths. All 11 MAGs capable of thiosulfate oxidation via the Sox system were affiliated with Pseudomonadota and exhibited abundance in the epilimnion of WLB (61.2 RPKM) and at, or above, the metalimnion of ELB (71.2 RPKM). In addition, the potential of sulfur mineralization was found in 96 MAGs, which were taxonomically diverse and distributed well across depth in both lobes. Most MAGs had cold-induced stress proteins. The capability of synthesizing exopolysaccharides was also detected across divergent phyla including Actinomycetota, Bacteroidota, Cyanobacteria, Gemmatimonadota, Myxococcota, Planctomycetota, Pseudomonadota, and Verrucomicrobiota. Only two MAGs belonging to Bacillota showed potential for spore formation, among which MAG62 belonging to *Virgibacillus* showed high abundance at the bottom sampling depth of the ELB.

Discussion

We used metagenomic approaches to show the distinct vertical distribution of major microbial metabolic potential, including carbon, nitrogen, and sulfur transformation within three physically and geochemically distinct zones of the WLB and ELB (Fig. 4). We recognize that although our metagenomic data capture a portion of the diversity and abundance of microbial genomes in the lake and contain key genes for specific processes, these data do not entirely ensure the complete microbial diversity or the functional activity of metabolic pathways. Accordingly, the aim of our study was to offer the dominant metabolic potentials for microbially driven biogeochemical processes in Lake Bonney.

Feeding by photoautotrophs and CO-oxidizers in the epilimnia

In environments with limited nutrient supply, photosynthetic autotrophs are crucial as major carbon sources and significantly impact lake ecosystems. Based on our data, *Pseudanabaena*, microalgae, and protists are expected to be the primary contributors to photosynthesis and carbon fixation in the epilimnia of Lake Bonney (Supplemental Fig. S2 and Table S10), where the supply of organic matter from allochthonous sources is greatly
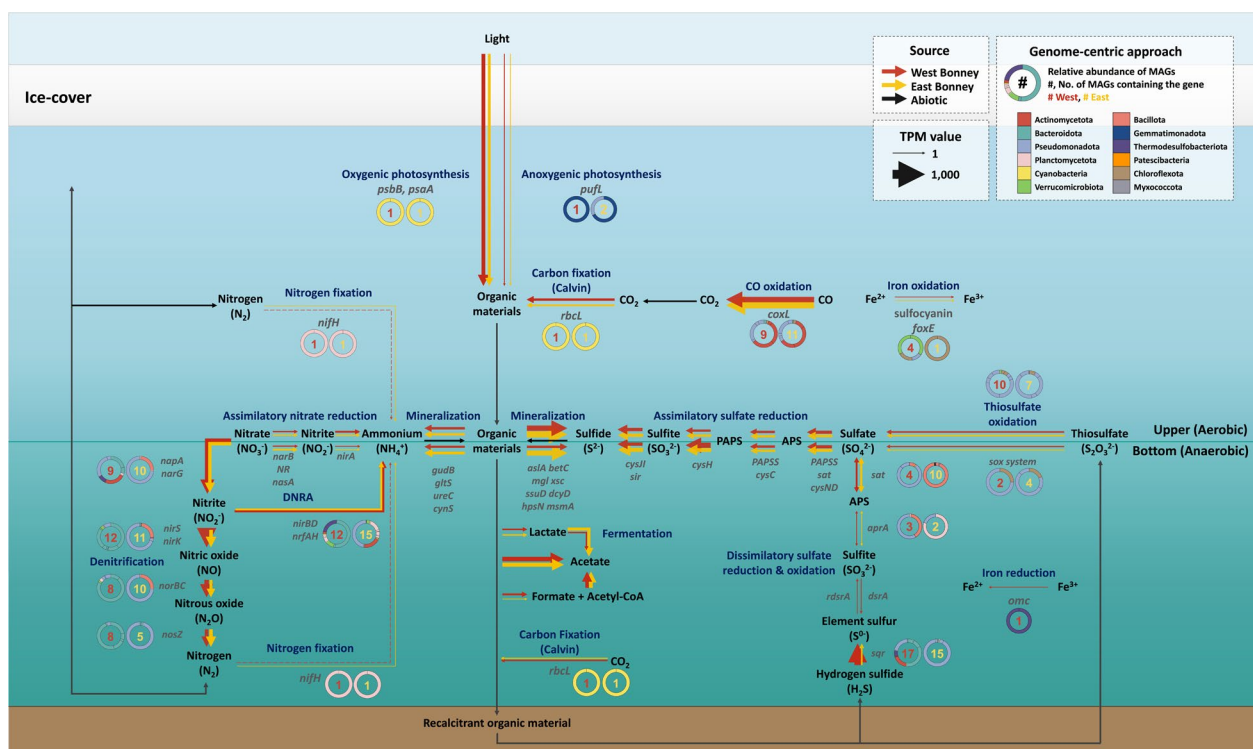
Fig. 4 Schematic of the nutrient cycling processes occurring in Lake Bonney based on our genomic data. Thicker arrows represent processes that are particularly abundant. The arrows are colored according to the sources

restricted due to the surrounding desert environment. Past research on Lake Bonney [53, 54] has shown that maximal biomass of phototrophs occurs immediately beneath the ice surface, where light is least limiting, and at the metalimnion, where the upward diffusion of nutrients supports metabolic activity [16]. Several studies have also confirmed that the highly shade-adapted phytoplankton support subsequent trophic levels [55–57]. Our data showed that the photosynthetic potential was higher in the epilimnion of WLB than ELB, likely due to the thinner ice cover in WLB resulting in higher PAR levels (Supplemental Fig. S1). Also, as previously reported by amplicon analysis, cyanobacteria were not dominant in Lake Bonney [10, 24], with *Chlamydomonas* and *Mychonastes* considered the primary photoautotrophs contributing to the lake's primary production (Supplemental Fig. S2) [24]. Although previous studies have reported the presence of cyanobacterial taxa including *Lyngbya*, *Oscillatoria*, *Nostoc*, and *Phormidium* spp., and demonstrated *Nostoc* sp. as a potentially diazotrophic cyanobacterium [58, 59], our study identified *Pseudanabaena* with no potential for atmospheric nitrogen fixation as the only cyanobacterium present.

In addition, we found that CO oxidation can be an alternative energy source to the Lake Bonney ecosystem. The potential for CO oxidation by carbon-monoxide dehydrogenase (CODH) was prevalent in both lobes of Lake Bonney being most abundant in the upper oxic layers (Fig. 2). CO-oxidizing microorganisms are diverse and can utilize CO as an electron donor under aerobic and anaerobic conditions [60–62]. Although multiple enzyme lineages for CODH have been reported, there is no clear relationship between their presence or specific types and the capacity for growth on CO [60, 62]. Consequently, in this study, MAGs possessing *coxL* (K03520) were assessed as potential CO-oxidizers. The dominant CO-oxidizing MAGs in Lake Bonney were *Acidimicrobiales*, *Nanopelagicales*, and *Burkholderiaceae*, which showed high abundance at the epilimnia of both lobes (Fig. 3). An earlier study in Ace Lake (Vestfold Hills, East Antarctica) also found evidence of microbial CO oxidation [63]. In oligotrophic environments like Lake Bonney, CO-oxidizers could employ the trace gas as a vital survival strategy. Their ubiquity in aerated aquatic ecosystems, coupled with the ability to readily diffuse CO into cells without requiring active transport, underscores the efficiency of this metabolic pathway in nutrient-limited settings [62]. Therefore, we propose that CO oxidation could be an alternative pathway for energy production in permanently ice-covered Antarctic lakes because it can serve as both carbon and electron sources for microorganisms, which could be a successful strategy for heterotrophs thriving in oligotrophic environments [60].

Rapid changes in microbial ecology at the metalimnia triggered by nutrient supply

Microbial structure and metabolic pathways change dramatically in the chemocline of the lake. Both lobes shared a common feature that the rapid decline in oxygen concentration was associated with an increase in the genomic potential of cytochrome c oxidase (*ccoN*) of the cbb_3 type, which has a higher oxygen affinity, and an elevation in the metabolic potential involved in anaerobic respiration. These physical and biological changes were more pronounced in WLB, which had a steeper chemocline.

There were also distinct nutrient cycles associated with the metalimnion of each lobe and were dependent upon the source of increased organic and inorganic compounds. An accumulation of nutrients in the metalimnion of ELB supplies nutrients to phototrophs, in contrast to the nutrient deficiency in the epilimnion [64]. Previous studies have also reported that Lake Bonney phytoplankton accumulate cellular chlorophyll levels as an adaptation to permanent low light conditions, contributing to the active growth of phototrophs [56]. Morgan-Kiss et al. [65] reported that the photochemical apparatus of Lake Bonney phytoplankton exhibits extreme shade adaptation to a permanent low-light environment enriched in blue–green wavelengths, which would contribute to the distribution of phototrophs in the lake. There was a concurrent increase in the potential for photosynthesis and carbon fixation, along with an elevated concentration of Chl-*a* at the metalimnion of ELB, indicating that phototrophic growth of algae and cyanobacteria exceeded cellular losses. However, in the metalimnion of the WLB, where a hypersaline and iron-rich glacial outflow flows in [66], there was a steep increase in Chl-*a* levels, while the potential for photosynthesis and carbon fixation decreased.

Although nutrients in ELB are supplied by nutrient accumulation and subsequent phototroph growth, and in WLB by both nutrient accumulation and inflow from Blood Falls, the rapid increase in nutrients in the metalimnia of both lobes supported higher abundances of bacteria, such as Flavobacteriaceae, that rely on phytoplankton-derived products (Fig. 3). As nutrients, such as sulfate, phosphate, POC, and PON, were supplied from the metalimnia (Supplemental Fig. S1), the potential for glycolysis, beta-oxidation, and glycoside hydrolase, representing properties of heterotrophs consuming these diverse nutrients, increased (Fig. 2).

Growth and survival strategies of microorganisms living in the hypersaline bottom water

The deep suboxic layers of Lake Bonney had more diverse metabolic potentials, including anaerobic respirations

driven by microbial metabolism under suboxic conditions and increased availability of metabolic substrates for anaerobic respiration (Fig. 4 and Supplemental Fig. S1). As expected, given diminishing sunlight with depth, heterotrophs predominated over autotrophs, supported by a lower potential for autotrophic carbon fixation and a higher potential for glycolysis, beta-oxidation, and fermentation (Fig. 2). At and below the metalimnia, primary production and accumulated nutrients may support the heterotrophic growth.

In the hypolimnion of the WLB, MAG34 (Flavobacteriaceae) and MAG72 (Acidimicrobiales), well-known heterotrophs, remained dominant as in the metalimnion, and were associated with a decrease in POC and an increase in DOC and DIC (Fig. 3 and Supplemental Fig. S1). Moreover, the anaerobic or oxygen-limited conditions could enable various microbes to utilize nitrogen and sulfur sources for their energy metabolism. Among the MAGs abundant at the hypolimnion of WLB, those belonging to Salinisphaeraceae (MAG109) and *Geopsychrobacter* (MAG87) showed potential for nitrate reduction via *narG* and/or *napA* genes. The hypersaline and iron-rich glacial outflow (Blood Falls; [13, 66]) that flows into and below the metalimnion of WLB could support microorganisms that can respire with sulfate and iron. Mikucki and Priscu [13] reported iron reduction in Blood Falls mediated by microorganisms, including *Shewanella frigidimarina* and *Geopsychrobacter electrodiphilus*. In our study, *Geopsychrobacter* sp. (MAG87), a member of the Thermodesulfobacteriota, was identified only from WLB and demonstrated a potential for iron reduction (Fig. 3). Based on redox potential, the energy yield from nitrate reduction is higher than from iron reduction. However, in the hypolimnion of WLB, where nitrate concentrations are very low, energy generation by iron-reducing bacteria is likely to dominate over nitrate reduction. Moreover, the genus *Geopsychrobacter* encompasses a variety of species, characterized as anaerobic, psychrotolerant, and predominantly found in saline environments [23]. The physiological characteristics and iron reduction capability of *Geopsychrobacter* sp. (MAG87) would provide an advantage for survival at the hypolimnion of WLB.

Halomonas sp. MAG115, a widely distributed genus throughout hypersaline environments [67], was highly abundant at the hypolimnion of the ELB. Previous studies suggested that the dominance of *Halomonas* spp. in hypersaline environments may be attributed to the rigidity of their cell wall composition, which protects the cell membrane from osmotic stress [67, 68]. The ability to withstand osmotic stress likely supports the high abundance of this MAG. *Virgibacillus* sp. (MAG62), belonging to a well-known halophilic bacterial genus, was also dominant at the hypolimnion of ELB. The ability to form dormant shapes may contribute to the survival of endospore-forming *Virgibacillus* under harsh conditions [69].

Deficient nitrogen and sulfur metabolism

Contemporary nitrogen metabolism in Lake Bonney is largely dependent on internal regeneration of ammonium deposited during the evolution of the lakes [21, 70, 71]. Although the MAGs classified to the genus *Mariniblastus* (MAG53 and MAG54) showed the potential for atmospheric nitrogen fixation, their abundance and the potential for the reaction (*nifH*) were very low. The high energy cost of the reaction is not conducive to nitrogen fixation in Lake Bonney. Additionally, the potential for nitrification was not detected in our study. Voytek et al. [72, 73] and Priscu et al. [21] reported the distribution of nitrifying bacteria above the chemocline and a central role of nitrification in the distribution of oxidized and reduced inorganic nitrogen in Lake Bonney. Although there were no genes involved in nitrification in both gene- and genome-centric datasets, the chemical profiles of NO_3^- and NO_2^- were entirely consistent with previous studies (Supplemental Fig. S1) [72, 73]. The discrepancy between our results and those of previous studies could result from seasonal change in the microbial populations [25], seasonal change in advected inflow [74], or methodological approaches used. Denitrifiers can use oxidized forms of nitrogen as terminal electron acceptors under oxygen-limiting conditions. Priscu [20] experimentally showed that denitrification of nitrate and nitrous oxide in the WLB is active whereas it was absent in ELB. However, Ward and Priscu [75] reported the presence of denitrifiers in both lobes of Lake Bonney, indicating that the apparent lack of denitrification in ELB is not due to the absence of bacteria capable of denitrification. We also identified MAGs with potential for denitrification, specifically *Virgibacillus* sp. (MAG62) and *Halomonas* sp. (MAG115) in the hypolimnion of ELB. Despite the detection of denitrifiers, the lack of measurable denitrification in ELB may be attributed to activity levels below experimental detection owing to the presence of high salt concentrations [23, 75].

The source of sulfur species could be supplied from sediment in both lobes and glacial outflow associated with Blood Falls in WLB [66, 76, 77]. In WLB, the inflow from Blood Falls, which is rich in sulfate, caused a sharp increase in sulfate concentration in the metalimnion (Supplemental Fig. S1). Although Mikucki and Priscu [13] reported high sulfur oxidation and sulfate production by *Thiomicrospira* sp. in Blood Falls, it was not observed in our study. Interestingly, the potential of hydrogen sulfide oxidation was highest in the hypolimnion of WLB. The

detection of the *sqr* gene, which utilizes hydrogen sulfide as a substrate, in either lobe of Lake Bonney where hydrogen sulfide has never been detected, suggests that the presence of the *sqr* gene may be attributed to nitrate reducing sulfide oxidizing bacteria (NRSOB). Among the 41 MAGs containing the *sqr* gene, 18 exhibited potentials for nitrate and/or nitrite reduction, with a notably high proportion of NRSOB capable of performing nitrite reduction. Specifically, the significant abundance of Acidimicrobiales (MAG72), Salinisphaeraceae (MAG109), Marinobacter (MAG114), and Gillisia (MAG32) at 30 m in the WLB could overestimate the potential for hydrogen sulfide oxidation. Except for the abundance of the *sqr* gene in WLB, our results infer that dissimilatory sulfate reduction and oxidation is very low. Our data further revealed that in ELB, the redox reaction between sulfate and sulfide is unlikely to occur or may occur infrequently due to the absence of *dsr* and *rdsr*. However, we found that MAGs possessing *dsr* or *sox* are usually dominant near the metalimnia (Supplemental Table S7). Some of these MAGs may respire nitrate, but almost all possessed cytochrome c oxidases, indicating that they are likely facultatively (an)aerobic. Therefore, the potential for redox reactions involving sulfur cannot be excluded, and the possibility of cryptic sulfur cycling driven by these microbes, which could oxidize sulfide using oxygen (or perhaps nitrate) in the oxygen-minimum zones of the metalimnia, cannot be ignored.

Conclusions

Our metagenomic analysis reveals the strategies microorganisms use to secure nutrients and energy across the diverse physicochemical zones of Lake Bonney. It further highlights the critical role of photoautotrophs, including algae and cyanobacteria, in the nutrient-scarce epilimnia, alongside the unique ecological niche that CO-oxidizing bacteria might occupy, which could support the ecosystem during the prolonged polar night by utilizing carbon monoxide for energy conservation. In the metalimnion of the ELB, upward diffusing nutrients allow photoautotrophs to flourish during summer despite low sunlight penetration (< 1% of incident during the summer). Organic matter produced by photosynthesis in this region enhanced the potential for heterotrophic metabolisms, as demonstrated by the increase in the potential for phototrophic and heterotrophic metabolisms inferred by our data. In contrast, in the metalimnion of WLB, the additional seasonal supply of nutrients by Blood Falls apparently meets the nutritional demand of heterotrophs and shapes a unique microbial community capable of iron reduction in the hypolimnion of WLB. This is particularly so in the hypolimnion of WLB, where nitrate concentrations are low, iron reduction can be a favorable microbial strategy. Notably, the potential for denitrification was prominent at the hypolimnion of WLB, especially with a high abundance of MAGs with the potential for nitrate reduction and sulfide oxidation. At the hypolimnion of the ELB, only two MAGs capable of resisting hypersaline stress were dominant. Collectively, our data underscore the complexity of microbial life in extreme environments, contributing significantly to our understanding of biogeochemical cycling in polar aquatic ecosystems.

Abbreviations

APS	Adenosine-5′-phosphosulfate
CBB	Calvin-Benson-Bassham
CODH	Carbon-monoxide dehydrogenase
DNRA	Dissimilatory nitrate reduction to ammonia
DO	Dissolved oxygen
DOC	Dissolved organic carbon
ED	Entner–Doudoroff
ELB	East lobe of Bonney
EMP	Embden–Meyerhof–Parnas
GH	Glycoside hydrolase
KO	KEGG orthology
MAGs	Metagenome-assembled genomes
MDVs	McMurdo Dry Valleys
ORFs	Open reading frames
PAR	Photosynthetically active radiation
POC	Particulate organic carbon
RPKM	Reads per kilobase of contig per million reads
RPM	Reads per million
WLB	West lobe of Bonney

Supplementary Information

The online version contains supplementary material available at https://doi.org/10.1186/s40793-024-00605-1.

Supplementary Material 1.

Supplementary Material 2.

Supplementary Material 3.

Supplementary Material 4.

Supplementary Material 5.

Supplementary Material 6.

Supplementary Material 7.

Supplementary Material 8.

Supplementary Material 9.

Supplementary Material 10.

Supplementary Material 11.

Supplementary Material 12.

Supplementary Material 13.

Supplementary Material 14.

Supplementary Material 15.

Supplementary Material 16.

Lee *et al. Environmental Microbiome*   (2024) 19:60

Page 13 of 15

Availability of data and materials
Metagenomic data are available in the NCBI with project ID PRJNA1044158. All MAGs analyzed in this study are also included under the same BioProject.

Declarations

Ethics approval and consent to participate
Not applicable.

Consent for publication
Not applicable.

Conflict of interests
The authors declare no competing interests.

Author details
[1]Division of Life Sciences, Korea Polar Research Institute, Yeonsu-Gu, Incheon 21990, Republic of Korea. [2]Department of Microbiology, Miami University, Oxford, OH 45056, USA. [3]Emeritus, Department of Land Resources and Environmental Sciences, Montana State University, Bozeman, MT 59717, USA.

References
1. Guo B, Li W, Santibáñez P, Priscu JC, Liu Y, Liu K. Organic matter distribution in the icy environments of Taylor Valley. Antarctica Sci Total Environ. 2022;841: 156639.
2. Obryk MK, Doran PT, Fountain AG, Myers M, McKay CP. Climate from the McMurdo Dry Valleys, Antarctica, 1986–2017: surface air temperature trends and redefined summer season. J Geophys Res Atmos. 2020;125:e2019JD032180.
3. Priscu JC, Wolf CF, Takacs CD, Fritsen CH, Laybourn-Parry J, Roberts EC, et al. Carbon transformations in a perennially ice-covered Antarctic lake. Bioscience. 1999;49:997–1008.
4. Obryk MK, Doran PT, Priscu JC. The permanent ice cover of Lake Bonney, Antarctica: the influence of thickness and sediment distribution on photosynthetically available radiation and chlorophyll-a distribution in the underlying water column. J Geophys Res-Biogeosci. 2014;119:1879–91.
5. Fritsen CH, Priscu JC. Seasonal change in the optical properties of the permanent ice cover on Lake Bonney, Antarctica: consequences for lake productivity and phytoplankton dynamics. Limnol Oceanogr. 1999;44:447–54.
6. Spigel RH, Priscu JC, Obryk MK, Stone W, Doran PT. The physical limnology of a permanently ice-covered and chemically stratified Antarctic lake using high resolution spatial data from an autonomous underwater vehicle. Limnol Oceanogr. 2018;63:1234–52.
7. Gooseff MN, Barrett JE, Adams BJ, Doran PT, Fountain AG, Lyons WB, et al. Decadal ecosystem response to an anomalous melt season in a polar desert in Antarctica. Nat Ecol Evol. 2017;1:1334–8.
8. Spigel RH, Priscu JC. Physical limnology of the McMurdo Dry Valleys lakes. In: Priscu JC, editor. Ecosystem dynamics in a polar desert: the McMurdo Dry Valleys, Antarctica. Washington: American Geophysical Union; 1998. p. 153–87.
9. Sherwell S, Kalra I, Li W, McKnight DM, Priscu JC, Morgan-Kiss RM. Antarctic lake phytoplankton and bacteria from near-surface waters exhibit high sensitivity to climate-driven disturbance. Environ Microbiol. 2022;24:6017–32.
10. Kwon M, Kim M, Takacs-Vesbach C, Lee J, Hong SG, Kim SJ, et al. Niche specialization of bacteria in permanently ice-covered lakes of the McMurdo Dry Valleys. Antarctica Environ Microbiol. 2017;19:2258–71.
11. Rojas-Jimenez K, Wurzbacher C, Bourne EC, Chiuchiolo A, Priscu JC, Grossart H-P. Early diverging lineages within Cryptomycota and Chytridiomycota dominate the fungal communities in ice-covered lakes of the McMurdo Dry Valleys. Antarctica Sci Rep. 2017;7:15348.
12. Vick-Majors TJ, Priscu JC, Amaral-Zettler AL. Modular community structure suggests metabolic plasticity during the transition to polar night in ice-covered Antarctic lakes. ISME J. 2014;8:778–89.
13. Mikucki JA, Priscu JC. Bacterial diversity associated with blood falls, a subglacial outflow from the Taylor Glacier. Antarctica Appl Environ Microbiol. 2007;73:4029–39.
14. Lawrence JP, Doran PT, Winslow LA, Priscu JC. Subglacial brine flow and wind-induced internal waves in Lake Bonney. Antarctica Antarct Sci. 2020;32:223–37.
15. Badgeley JA, Pettit EC, Carr CG, Tulaczyk S, Mikucki JA, Lyons WB, Team MS. An englacial hydrologic system of brine within a cold glacier: Blood Falls, McMurdo Dry Valleys. Antarctica J Glaciol. 2017;63:387–400.
16. Priscu JC. Phytoplankton nutrient deficiency in lakes of the McMurdo dry valleys. Antarctica Freshw Biol. 1995;34:215–27.
17. Dore JE, Priscu JC. Phytoplankton phosphorus deficiency and alkaline phosphatase activity in the McMurdo Dry Valley lakes. Antarctica Limnol Oceanogr. 2001;46:1331–46.
18. Vick TJ, Priscu JC. Bacterioplankton productivity in lakes of the Taylor Valley, Antarctica, during the polar night transition. Aquat Microb Ecol. 2012;68:77–90.
19. Lee PA, Priscu JC, DiTullio GR, Riseman SF, Tursich N, de Mora SJ. Elevated levels of dimethylated-sulfur compounds in Lake Bonney, a poorly ventilated Antarctic lake. Limnol Oceanogr. 2004;49:1044–55.
20. Priscu JC. The biogeochemistry of nitrous oxide in permanently ice-covered lakes of the McMurdo Dry Valleys. Antarctica Glob Change Biol. 1997;3:301–15.
21. Priscu JC, Christner BC, Dore JE, Westley MB, Popp BN, Casciotti KL, Lyons WB. Supersaturated N_2O in a perennially ice-covered Antarctic lake: molecular and stable isotopic evidence for a biogeochemical relict. Limnol Oceanogr. 2008;53:2439–50.
22. Ward BB, Granger J, Maldonado MT, Casciotti KL, Harris S, Wells ML. Denitrification in the hypolimnion of permanently ice-covered Lake Bonney. Antarctica Aquatic Microbial Ecology. 2005;38:295–307.
23. Lee PA, Mikucki JA, Foreman CM, Priscu JC, DiTullio GR, Riseman SF, et al. Thermodynamic constraints on microbially mediated processes in lakes of the McMurdo Dry Valleys. Antarctica Geomicrobiol J. 2004;21:221–37.
24. Li W, Morgan-Kiss RM. Influence of environmental drivers and potential interactions on the distribution of microbial communities from three permanently stratified Antarctic lakes. Front Microbiol. 2019;10:1067.
25. Bowman JS, Vick-Majors TJ, Morgan-Kiss R, Takacs-Vesbach C, Ducklow HW, Priscu JC. Microbial community dynamics in two polar extremes: the lakes of the McMurdo Dry Valleys and the West Antarctic Peninsula marine ecosystem. Bioscience. 2016;66:829–47.
26. Takacs-Vesbach C, Zeglin L, Barrett JE, Gooseff MN, Priscu JC, Doran P, Lyons WB. Factors promoting microbial diversity in the McMurdo Dry Valleys, Antarctica. In: Doran PT, Lyons WB, McKnight DM, editors. Life in Antarctic Deserts and other cold dry environments: astrobiological Analogs. Cambridge: Cambridge University Press; 2010. p. 221.
27. Takacs CD, Priscu JC, McKnight DM. Bacterial dissolved organic carbon demand in McMurdo Dry Valley lakes. Antarctica Limnol Oceanogr. 2001;46:1189–94.
28. Bolger AM, Lohse M, Usadel B. Trimmomatic: a flexible trimmer for Illumina sequence data. Bioinformatics. 2014;30:2114–20.
29. Li H, Durbin R. Fast and accurate short read alignment with Burrows-Wheeler transform. Bioinformatics. 2009;25:1754–60.
30. Li D, Luo R, Liu C-M, Leung C-M, Ting H-F, Sadakane K, et al. MEGAHIT v1. 0: a fast and scalable metagenome assembler driven by advanced methodologies and community practices. Methods. 2016;102:3–11.

Lee *et al. Environmental Microbiome*   (2024) 19:60

Page 14 of 15

31. Hyatt D, Chen G-L, LoCascio PF, Land ML, Larimer FW, Hauser LJ. Prodigal: prokaryotic gene recognition and translation initiation site identification. BMC Bioinform. 2010;11:1–11.
32. Mao X, Cai T, Olyarchuk JG, Wei L. Automated genome annotation and pathway identification using the KEGG Orthology (KO) as a controlled vocabulary. Bioinformatics. 2005;21:3787–93.
33. Rawlings ND, Barrett AJ, Bateman A. MEROPS: the peptidase database. Nucleic Acids Res. 2010;38:D227–33.
34. Garber AI, Nealson KH, Okamoto A, McAllister SM, Chan CS, Barco RA, Merino N. FeGenie: a comprehensive tool for the identification of iron genes and iron gene neighborhoods in genome and metagenome assemblies. Front Microbiol. 2020;11: 499513.
35. Tully BJ, Wheat CG, Glazer BT, Huber JA. A dynamic microbial community with high functional redundancy inhabits the cold, oxic subseafloor aquifer. ISME J. 2018;12:1–16.
36. Dahl C, Engels S, Pott-Sperling AS, Schulte A, Sander J, Lübbe Y, et al. Novel genes of the dsr gene cluster and evidence for close interaction of Dsr proteins during sulfur oxidation in the phototrophic sulfur bacterium Allochromatium vinosum. J Bacteriol. 2005;187:1392–404.
37. Thompson JD, Higgins DG, Gibson TJ. CLUSTAL W: improving the sensitivity of progressive multiple sequence alignment through sequence weighting, position-specific gap penalties and weight matrix choice. Nucleic Acids Res. 1994;22:4673–80.
38. Stamatakis A. RAxML version 8: a tool for phylogenetic analysis and post-analysis of large phylogenies. Bioinformatics. 2014;30:1312–3.
39. Darriba D, Posada D, Kozlov AM, Stamatakis A, Morel B, Flouri T. ModelTest-NG: a new and scalable tool for the selection of DNA and protein evolutionary models. Mol Biol Evol. 2020;37:291–4.
40. Langmead B, Salzberg SL. Fast gapped-read alignment with Bowtie 2. Nat Methods. 2012;9:357–9.
41. Alneberg J, Sundh J, Bennke C, Beier S, Lundin D, Hugerth LW, et al. BARM and BalticMicrobeDB, a reference metagenome and interface to meta-omic data for the Baltic Sea. Sci Data. 2018;5: 180146.
42. Wu YW, Simmons BA, Singer SW. MaxBin 2.0: an automated binning algorithm to recover genomes from multiple metagenomic datasets. Bioinformatics. 2016;32:605–7.
43. Kang DD, Li F, Kirton E, Thomas A, Egan R, An H, Wang Z. MetaBAT 2: an adaptive binning algorithm for robust and efficient genome reconstruction from metagenome assemblies. PeerJ. 2019;7: e7359.
44. Alneberg J, Bjarnason BS, De Bruijn I, Schirmer M, Quick J, Ijaz UZ, et al. Binning metagenomic contigs by coverage and composition. Nat Methods. 2014;11:1144–6.
45. Sieber CM, Probst AJ, Sharrar A, Thomas BC, Hess M, Tringe SG, Banfield JF. Recovery of genomes from metagenomes via a dereplication, aggregation and scoring strategy. Nat Microbiol. 2018;3:836–43.
46. Olm MR, Brown CT, Brooks B, Banfield JF. dRep: a tool for fast and accurate genomic comparisons that enables improved genome recovery from metagenomes through de-replication. ISME J. 2017;11:2864–8.
47. Parks DH, Imelfort M, Skennerton CT, Hugenholtz P, Tyson GW. CheckM: assessing the quality of microbial genomes recovered from isolates, single cells, and metagenomes. Genome Res. 2015;25:1043–55.
48. Bowers RM, Kyrpides NC, Stepanauskas R, Harmon-Smith M, Doud D, Reddy TBK, et al. Minimum information about a single amplified genome (MISAG) and a metagenome-assembled genome (MIMAG) of bacteria and archaea. Nat Biotechnol. 2017;35:725–31.
49. Chaumeil P-A, Mussig AJ, Hugenholtz P, Parks DH. GTDB-Tk: a toolkit to classify genomes with the Genome Taxonomy Database. Oxford: Oxford University Press; 2020.
50. Kumar S, Stecher G, Li M, Knyaz C, Tamura K. MEGA X: molecular evolutionary genetics analysis across computing platforms. Mol Biol Evol. 2018;35:1547.
51. Letunic I, Bork P. Interactive Tree Of Life (iTOL) v5: an online tool for phylogenetic tree display and annotation. Nucleic Acids Res. 2021;49:W293–6.
52. Graham E, Heidelberg J, Tully B. Potential for primary productivity in a globally-distributed bacterial phototroph. ISME J. 2018;12:1861–6.
53. Lizotte MP, Priscu JC. Photosynthesis irradiance relationships in phytoplankton from the physically stable water column of a perennially ice-covered lake (Lake Bonney, Antarctica). J Phycol. 1992;28:179–85.
54. Dolhi JM, Teufel AG, Kong WD, Morgan-Kiss RM. Diversity and spatial distribution of autotrophic communities within and between ice-covered Antarctic lakes (McMurdo Dry Valleys). Limnol Oceanogr. 2015;60:977–91.
55. Bayliss P, Ellis-Evans JC, Laybourn-Parry J. Temporal patterns of primary production in a large ultra-oligotrophic Antarctic freshwater lake. Polar Biol. 1997;18:363–70.
56. Morgan-Kiss R, Lizotte M, Kong W, Priscu J. Photoadaptation to the polar night by phytoplankton in a permanently ice-covered Antarctic lake. Limnol Oceanogr. 2016;61:3–13.
57. Patriarche JD, Priscu JC, Takacs-Vesbach C, Winslow L, Myers KF, Buelow H, et al. Year-round and long-term phytoplankton dynamics in Lake Bonney, a permanently ice-covered Antarctic Lake. J Geophys Res-Biogeosciences. 2021;126:e202JG005925.
58. Paerl HW, Priscu JC. Microbial phototrophic, heterotrophic, and diazotrophic activities associated with aggregates in the permanent ice cover of Lake Bonney. Antarctica Microbial Ecology. 1998;36:221–30.
59. Wing K, Priscu J. Microbial communities in the permanent ice cap of Lake Bonney, Antarctica: relationships among chlorophyll a, gravel and nutrients. Antarct J US. 1993;28:246–9.
60. King GM, Weber CF. Distribution, diversity and ecology of aerobic CO-oxidizing bacteria. Nat Rev Microbiol. 2007;5:107–18.
61. Meyer O, Fiebig K. Enzymes oxidizing carbon monoxide. In: Degn H, Cox RP, Toftlund H, editors. Gas enzymology. Dordrecht: Springer; 1985. p. 147–68.
62. Greening C, Grinter R. Microbial oxidation of atmospheric trace gases. Nat Rev Microbiol. 2022;20:513–28.
63. Lauro FM, DeMaere MZ, Yau S, Brown MV, Ng C, Wilkins D, et al. An integrative study of a meromictic lake ecosystem in Antarctica. ISME J. 2011;5:879–95.
64. Leach TH, Beisner BE, Carey CC, Pernica P, Rose KC, Huot Y, et al. Patterns and drivers of deep chlorophyll maxima structure in 100 lakes: the relative importance of light and thermal stratification. Limnol Oceanogr. 2018;63:628–46.
65. Morgan-Kiss RM, Priscu JC, Pocock T, Gudynaite-Savitch L, Huner NP. Adaptation and acclimation of photosynthetic microorganisms to permanently cold environments. Microbiol Mol Biol Rev. 2006;70:222–52.
66. Mikucki JA, Foreman CM, Sattler B, Berry Lyons W, Priscu JC. Geomicrobiology of Blood Falls: an iron-rich saline discharge at the terminus of the Taylor Glacier. Antarctica Aquat Geochem. 2004;10:199–220.
67. Joulak I, Finore I, Nicolaus B, Leone L, Moriello AS, Attia H, et al. Evaluation of the production of exopolysaccharides by newly isolated Halomonas strains from Tunisian hypersaline environments. Int J Biol Macromol. 2019;138:658–66.
68. Peng S, Kai M, Yang X, Luo Y, Bai L. Study on the osmoregulation of "Halomonas socia" NY-011 and the degradation of organic pollutants in the saline environment. Extremophiles. 2020;24:843–61.
69. Gray DA, Dugar G, Gamba P, Strahl H, Jonker MJ, Hamoen LW. Extreme slow growth as alternative strategy to survive deep starvation in bacteria. Nat Commun. 2019;10:890.
70. Priscu JC, Vincent WF, Howard-Williams C. Inorganic nitrogen uptake and regeneration in perennially icecovered Lakes Fryxell and Vanda. Antarctica J Plankton Res. 1989;11:335–51.
71. Priscu JC. Phytoplankton nutrient deficiency in lakes of the McMurdo dry valleys. Antarctica Freshwater Biol. 1995;34:215–27.
72. Voytek MA, Priscu JC, Ward BB. The distribution and relative abundance of ammonia-oxidizing bacteria in lakes of the McMurdo Dry Valley. Antarctica Hydrobiol. 1999;401:113–30.
73. Voytek MA, Ward BB, Priscu JC. The abundance of ammonium-oxidizing bacteria in Lake Bonney, Antarctica determined by immunofluorescence, Pcr and in situ hybridization. In: Priscu JC, editor. Ecosystem dynamics in a polar desert: the Mcmurdo Dry Valleys, Antarctica. Washington: American Geophysical Union; 1998. p. 217–28.
74. Gooseff MN, Barrett JE, Adams BJ, Doran PT, Fountain AG, Lyons WB, et al. Decadal ecosystem response to an anomalous melt season in a polar desert in Antarctica. Nat Ecol Evolution. 2017;1:1334–8.
75. Ward BB, Priscu JC. Detection and characterization of denitrifying bacteria from a permanently ice-covered Antarctic lake. Hydrobiologia. 1997;347:57–68.
76. Wadham JL, De'Ath R, Monteiro F, Tranter M, Ridgwell A, Raiswell R, Tulaczyk S. The potential role of the Antarctic Ice Sheet in global biogeochemical cycles. Earth Environ Sci Trans R Soc Edinb. 2013;104:55–67.

Lee *et al. Environmental Microbiome*   (2024) 19:60

Page 15 of 15

77. Gill-Olivas B, Telling J, Tranter M, Skidmore M, Christner B, O'Doherty S, Priscu J. Subglacial erosion has the potential to sustain microbial processes in Subglacial Lake Whillans. Antarctica Commun Earth Environ. 2021;2:134.

Publisher's Note